Biophysical Chemistry 136 (2008) 87–95

Contents lists available at ScienceDirect

Biophysical Chemistry

journal homepage: http://www.elsevier.com/locate/biophyschem

Dynamic simulation of the effect of calcium-release activated calcium channel on cytoplasmic Ca^{2+} oscillation

Xiao-fang Chen, Cong-xin Li, Peng-ye Wang, Ming Li, Wei-chi Wang *

Laboratory of Soft Matter Physics, Beijing National Laboratory for Condensed Matter Physics, Institute of Physics, Chinese Academy of Sciences, Beijing 100080, China

ARTICLE INFO

Article history:
Received 4 March 2008
Received in revised form 28 April 2008
Accepted 28 April 2008
Available online 6 May 2008

Keywords:
Calcium oscillations
Orai1
STIM1
SOC channel
CRAC

ABSTRACT

A mathematical model is proposed to illustrate the activation of STIM1 (stromal interaction molecule 1) protein, the assembly and activation of calcium-release activated calcium (CRAC) channels in T cells. In combination with De Young–Keizer–Li–Rinzel model, we successfully reproduce a sustained Ca^{2+} oscillation in cytoplasm. Our results reveal that Ca^{2+} oscillation dynamics in cytoplasm can be significantly affected by the way how the Orai1 CRAC channel are assembled and activated. A low sustained Ca^{2+} influx is observed through the CRAC channels across the plasma membrane. In particular, our model shows that a tetrameric channel complex can effectively regulate the total quantity of the channels and the ratio of the active channels to the total channels, and a period of Ca^{2+} oscillation about 29 s is in agreement with published experimental data. The bifurcation analyses illustrate the different dynamic properties between our mixed Ca^{2+} feedback model and the single positive or negative feedback models.

1. Introduction

Calcium (Ca^{2+}) oscillations regulate a series of biological events including gene transcription, protein synthesis, protein degradation, apoptosis, necrosis and exocytosis, etc [1–3]. The oscillations are based mainly on an influx of Ca^{2+} into the cytoplasm through activated inositol 1,4,5-trisphosphate receptors (IP_3R) in the endoplasmic reticulum (ER) membrane. A number of theoretical models have been proposed previously to describe the Ca^{2+} dynamics in cytoplasm [4–16]. In an original model proposed by Meyer and Stryer, cooperativity and positive feedback between cytoplasmic Ca^{2+} and IP_3 give rise to the repetitive Ca^{2+} spiking [8]. A two-pool model by Goldbetter et al. predicts the cytoplasmic Ca^{2+} oscillation based on Ca^{2+}-induced Ca^{2+} release (CICR) while the concentration of IP_3 is taken as certain fixed values [9]. Moreover, a simple one-pool model by Somogyi and Stucki is in agreement well with the experimental data for hormone-induced Ca^{2+} oscillation in hepatocytes [10]. In terms of experimental data from *Xenopus laevis* oocytes, Atri et al. proposed a biphasic pattern of IP_3R where the Ca^{2+} channel is facilitated by moderate concentration of cytoplasmic Ca^{2+} and inhibited by high cytoplasmic Ca^{2+} [11]. The De Young–Keizer model allows a random binding of Ca^{2+} and IP_3 molecules to each subunit [5]. A refined electrochemical model constructed by Marhl et al. provides us a different viewpoint to describe the cytoplasmic Ca^{2+} dynamics [14]. The theoretical modeling and analyzing have been thoroughly reviewed in [15] and [16].

In many cases, continuing Ca^{2+} entry across the plasma membrane (PM) is required to prevent the net loss of ER Ca^{2+} store and to maintain ongoing signaling [17]. Experiments show that Ca^{2+} entry is partially controlled by the level of Ca^{2+} in agonist-sensitive intracellular stores [18]. The phenomenon, now called "store-operated Ca^{2+} entry" (SOCE) is commonly supported from experimental data in many types of excitable and non-excitable cells [19]. Physiologically, SOCE results from the stimulation of cell surface receptors that activates the specific phospholipase C (PLC) isoforms. PLC then catalyzes the production of inositol 1,4,5-trisphosphate (IP_3), which triggers the Ca^{2+} release through IP_3R. Finally, the store-operated channels (SOCs) in plasma membrane (PM) are activated to mediate the Ca^{2+} influx. In addition, SOCE allows sustained Ca^{2+} oscillation over extended periods and other Ca^{2+}-dependent events in response to prolonged stimulation [20,21]. A store-operated Ca^{2+} current, named Ca^{2+}-release-activated Ca^{2+} (CRAC) current (I_{CRAC}) is the clearest evidence of SOCE in mast cells and T cells [22–24]. I_{CRAC} is triggered in T cells or mast cells by physiological stimulation through T cell receptors or immunoglobulin-E receptor or by depletion of Ca^{2+} store. I_{CRAC} is also triggered passively by depletion of ER Ca^{2+} store in the presence of chelators [25]. Generally, I_{CRAC} enables a low sustained Ca^{2+} influx over minutes to hours, and thus control the transcription of cytokine genes in T cells [26]. Then a low conductance of CRAC channels has a small influx of Ca^{2+}.

However, the linking between SOCE, the fluctuation in cytoplasmic Ca^{2+}, and the depletion and refilling of ER Ca^{2+} store have long eluded a detailed description for over two decades. Recently, the breakthroughs have been achieved experimentally that the Ca^{2+} entry in plasma membrane is related to two proteins, STIM1 and Orai1. STIM1 protein is the Ca^{2+} sensor mostly found in ER membrane [27–30], and Orai1 is the essential component of the SOCE channel located in the plasma membrane [31–37]. When the concentration of ER Ca^{2+} ($[Ca^{2+}]_{ER}$) is sufficient high, the EF-hand site in STIM1 is occupied by Ca^{2+},

* Corresponding author. Tel.: +86 10 8264 9497; fax: +86 10 8264 0224.
E-mail address: weichi@aphy.iphy.ac.cn (W. Wang).

0301-4622/$ – see front matter © 2008 Elsevier B.V. All rights reserved.
doi:10.1016/j.bpc.2008.04.010

therefore the STIM1 luminal domain is in its resting conformation. Upon the depletion of ER luminal Ca^{2+}, bound Ca^{2+} dissociates from the EF-hand. It may induce a conformation change of the STIM1 luminal domain and leads to the variation of the protein–protein interactions. The activated STIM1 moves laterally in ER membrane to the specific gap junction where Orai1 proteins gather oppositely in plasma membrane. Due to the activation by STIM1, the CRAC channel will be opened, mediating the Ca^{2+} influx across the plasma membrane. Researchers have recently modeled the communications between the ER Ca^{2+} and the store-operated calcium channels (SOCs) by a Ca^{2+} influx factor [38]. To the best of our knowledge, there has been no theoretical model to investigate the coupling of the STIM1 activations with the assembly and activation of CRAC channel in cytoplasmic Ca^{2+} oscillations in T cells.

Here, due to the complexity of non-excitable cells, our model focuses only on several types of non-excitable cells, especially on T cells to study the effect of CRAC channel on the cytoplasmic Ca^{2+} oscillations. We assume that the STIM1 forms a dimer which has no affinity to Orai1 CRAC channels. When ER Ca^{2+} decreases, two Ca^{2+} ions dissociate cooperatively from STIM1 dimer. The formed apoSTIM1 dimers can activate the Orai1 CRAC channels. The Orai1 CRAC channels function as the main pores for the Ca^{2+} entry in T cells, while the Ca^{2+} leak from extracellular medium to cytoplasm across plasma membrane is, on the other hand, subsidiary. We further assume that several Orai1 subunits constitute a multimeric Ca^{2+} channel (CRAC channels) in a cooperative way on plasma membrane prior to its activation. Upon activation, the CRAC channels are opened to mediate the Ca^{2+} entry in plasma membrane.

In the present work, a dynamic model is briefly introduced to describe the activation of STIM1 protein, the assembly and activation of Orai1 CRAC channels. Combining with the simplified De Young–Keizer–Li–Rinzel model, we can quantitatively analyze the cytoplasmic Ca^{2+} oscillation, and the closing and opening of CRAC channels in plasma membrane. We found that a tetrameric Orai1 CRAC channel can effectively control the period of the cytoplasmic Ca^{2+} oscillation. We also observed that our Ca^{2+} dynamic system still keeps frequency-modulated characteristics as proposed by previous study [4]. Using our mixed feedback model, we further investigated the feedback effect of Ca^{2+} on the inositol 1,4,5-trisphosphate (IP_3) production. The bifurcation analyses were performed to compare the dynamic behaviors of the mixed feedback model with the single negative and positive feedback model.

2. Model description

Taking the effect of CRAC channels into account, we have studied the Ca^{2+} oscillation dynamics in T cells. For simplicity, we have only considered that the cytoplasmic Ca^{2+} has two main sources: one from internal store located in the ER; the other from extracellular pool. There is a sharp gradient across the plasma membrane. Generally, the concentration of the cytoplasmic Ca^{2+} ($[Ca^{2+}]_{cyt}$) is about 0.1 μM in resting state, while the extracellular Ca^{2+} concentration ($[Ca^{2+}]_{EC}$) is permanently close to 10,000 times higher. Under these circumstances, we assume that there exists a very small Ca^{2+} leak in plasma membrane from outside of the cell to cytoplasm. The Ca^{2+} oscillation is totally abolished with this low Ca^{2+} leak alone.

The IP_3 receptor (IP_3R), sarcoplasmic/endoplasmic reticulum calcium ATPase (SERCA), and STIM1 proteins are mostly located in ER membrane. The IP_3R opens upon arrival of the signals. Then, the ER Ca^{2+} is released into the cytoplasm. When $[Ca^{2+}]_{cyt}$ increases, the SERCA pumps transfer Ca^{2+} from the cytoplasm into the ER. Meanwhile the plasma membrane calcium ATPases (PMCA) transport Ca^{2+} from cytoplasm to extracellular pool. Under the effects of SERCA and PMCA, $[Ca^{2+}]_{cyt}$ returns to its resting level.

A nine-variable model developed by De Young and Keizer is the first theoretical model to describe the microscopic kinetics of IP_3R in the ER membrane [5]. Li and Rinzel proposed a simplified two-variable version which resembles the Hodgkin–Huxley model of electrical excitability in plasma membrane [6]. In an open system, the balance of the cytoplasmic Ca^{2+} depends on the net fluxes in both ER membrane and plasma membrane. The fundamental kinetic equations of Ca^{2+} oscillation are described as follows:

$$\frac{d[Ca^{2+}]_{cyt}}{dt} = (J_{ERchannel} - J_{SERCA}) + (J_{PMchannel} - J_{PMCA}), \tag{1}$$

$$\frac{d[Ca^{2+}]_{ER}}{dt} = \frac{1}{\alpha}(J_{SERCA} - J_{ERchannel}), \tag{2}$$

$$\frac{d[IP_3]_{cyt}}{dt} = v_{PLC} - v_{deg}, \tag{3}$$

$$\frac{dh}{dt} = A\left[K_d - \left([Ca^{2+}]_{cyt} + K_d\right)h\right]. \tag{4}$$

Eqs. (1)–(3) are the dynamic simulations for the cytoplasmic Ca^{2+}, the ER Ca^{2+} and the cytoplasmic IP_3 concentrations, respectively. Eq. (4) represents the fraction of IP_3R channels not inactivated by Ca^{2+} and available to open. $J_{ERchannel}$ and $J_{PMchannel}$ are the total flux through the ER membrane and plasma membrane Ca^{2+} channel, respectively. J_{SERCA} and J_{PMCA} are the total Ca^{2+} flux through the SERCA and PMCA pumps, respectively [4,39–41]. Their expressions are given in the following paragraphs. The parameters of α, A, K_d are listed in Table 1 according to published results with some modifications [4,6,39,41]. Bifurcation dynamics were analyzed using XPPAUT software package.

2.1. IP_3 dynamics

The production of phospholipase C isoforms (i.e. PLCβ) depends on $[Ca^{2+}]_{cyt}$ [4,45]

$$v_{PLC} = V_{PLC}\frac{[Ca^{2+}]_{cyt}^2}{K_{PLC}^2 + [Ca^{2+}]_{cyt}^2}, \tag{5}$$

Where, V_{PLC} is the maximal production rate of PLC isoforms, K_{PLC} is the sensitivity of PLC to Ca^{2+}. Here PLC's activities are cooperatively regulated by $[Ca^{2+}]_{cyt}$. The production of IP_3 catalyzed by PLC is thus under the positive feedback effect of the cytoplasmic Ca^{2+}.

IP_3 is degraded through phosphorylation by IP_3 kinases (i.e. IP_3K). The kinetic equation can be written as

$$v_{deg} = k_{deg}\frac{[Ca^{2+}]_{cyt}^2}{K_{deg}^2 + [Ca^{2+}]_{cyt}^2}[IP_3]_{cyt}, \tag{6}$$

Where, k_{deg} represents the phosphorylation rate constants, K_{deg} is the half-saturation constant of IP_3 kinases. We write the kinetic equation for the IP_3 production in the following form according to Höfer model with some modifications [4]

$$\begin{aligned}\frac{d[IP_3]_{cyt}}{dt} &= v_{PLC} - v_{deg} \\ &= V_{PLC}\frac{[Ca^{2+}]_{cyt}^2}{K_{PLC}^2 + [Ca^{2+}]_{cyt}^2} - k_{deg}\frac{[Ca^{2+}]_{cyt}^2}{K_{deg}^2 + [Ca^{2+}]_{cyt}^2}[IP_3]_{cyt}.\end{aligned} \tag{7}$$

When K_{PLC} equals to zero ($K_{PLC}=0$, $K_{deg}\neq 0$), we obtain a negative feedback of $[Ca^{2+}]_{cyt}$ on IP_3 metabolism. When K_{deg} is equal to zero ($K_{PLC}\neq 0$, $K_{deg}=0$), it stands for a positive feedback and the second term in Eq. (7) degenerates thus to be a linear function independent of the cytoplasmic Ca^{2+} fluctuation. In this paper, we prefer to discuss IP_3 dynamics in such a way that K_{PLC} and K_{deg} are all not equal to zero ($K_{PLC}\neq 0$, $K_{deg}\neq 0$). We describe it as a mixed feedback of the cytoplasmic Ca^{2+} on IP_3 production.

Table 1
Parameters of the model

Parameter	Value	Description
α	0.185	Ratio of effective volumes for ER/cytoplasm
A	0.5 s^{-1}	Variable to control the relative time scale between differential equations
K_d	0.4 μM	Dissociation constants of Ca^{2+}-inavtivation sites on IP_3R
V_{PLC}	0.5 μM s^{-1}	Maximal rate of IP_3 production
K_{PLC}	0.12 μM	Half-activation constant of PLC
k_{deg}	0.5 s^{-1}	IP_3 degradation rate constant mainly through phosphorylation
K_{deg}	0.1 μM	Half-activation constant of IP_3 kinases
L	$9.3\times10^{-4}s^{-1}$	Ca^{2+} leak from ER to cytoplasm
P_{IP3R}	66.6 s^{-1}	Maximal total permeability of IP_3 channels
K_i	1.0 μM	Dissociation constant of IP_3 sites on IP_3R
K_a	0.4 μM	Dissociation constant of Ca^{2+}-activation sites on IP_3R
K_{PMleak}	$5\times10^{-7}s^{-1}$	Leakage of Ca^{2+} from extracellular pool to intracellular
k_{soc}	2.3 s^{-1} μM^{-1}	Rate constant of Ca^{2+} through CRAC channels
$[Ca^{2+}]_{ec}$	1500 μM	Extracellular concentration of Ca^{2+}
K_1	5 μM	Apparent dissociation constant of ER Ca^{2+} to STIM1 dimers
k_a	4 s^{-1}	Maximal production rate of apoSTIM1 dimers
k_i	6 s^{-1}	Degradation rate constant of apoSTIM1 dimers
K_2	0.14 μM	Apparent dissociation constant for oligomers
V_{S_4}	0.25 μM s^{-1}	Maximal production rate of apoSTIM1 oligomers
k_d	0.8 s^{-1}	Degradation rate constant of apoSTIM1 oligomers
V_{cp}	0.18 nM s^{-1}	Maximal production rate of closed CRAC channels
K_c	0.02 nM	Half-activation constant
k_{dc}	0.5 s^{-1}	Degradation rate constant of closed CRAC channels
k_{op}	0.5 μM s^{-1}	Maximal production rate of opened CRAC channels
K_o	0.2 μM	Half-activation constant
k_{od}	1 s^{-1}	Turning rate of opened CRAC channels to closed channels
k_{do}	0.6 s^{-1}	Degradation rate constant of opened CRAC channels
$STIM1_{tot}$	0.6 μM	Total STIM1 dimers
$Orai1_{tot}$	1 nM	Total Orai1 subunits
l	1	Stoichiometric number of the interactions of STIM1 dimer with CRAC channels
n	1 2, 3	Hill coefficient of the formation of closed CRAC channels
r	1 3, 4	Orai1 number to form CRAC channels
V_{SERCA}	1 μM s^{-1}	Maximum flux across SERCA
V_{PMCA}	1 μM s^{-1}	Maximum flux across PMCA
K_{SERCA}	0.15 μM	SERCA activation constant
K_{PMCA}	0.45 μM	PMCA activation constant
p	2	SERCA Hill coefficient
q	2	PMCA Hill coefficient

2.2. IP_3 receptor/channel and Ca^{2+} pumps

It is suggested that the IP_3 receptor (IP_3R) consists of four identical subunits. Each subunit has one IP_3 binding site and two Ca^{2+} binding sites, one for activation, the other for inhibition. The channel activity is cooperatively regulated by the binding–unbinding of IP_3 and Ca^{2+} at these binding sites.

In our model, $J_{ERchannel}$ is given by Eq. (8) according to [41]

$$J_{ERchannel}=\left[L+\frac{P_{IP3R}[IP_3]_{cyt}^3[Ca^{2+}]_{cyt}^3h^3}{\left([IP_3]_{cyt}+K_i\right)^3\left([Ca^{2+}]_{cyt}+K_a\right)^3}\right]\left([Ca^{2+}]_{ER}-[Ca^{2+}]_{cyt}\right), \tag{8}$$

Where, L is the ER leak permeability and P_{IP3R} is the maximum total permeability of IP_3 channels. K_i and K_a are the dissociation constants of IP_3, Ca^{2+}-activation sites on the IP_3R.

Two Ca^{2+} pumps, SERCA and PMCA locate in the ER membrane and the plasma membrane, respectively. They transfer Ca^{2+} against the concentration gradient in the presence of ATP. The kinetic equations of the pumps are given according to [39]. The parameters V_{SERCA}, V_{PMCA}, K_{SERCA}, K_{PMCA}, p and q are listed in Table 1.

$$J_{SERCA}=V_{SERCA}\frac{[Ca^{2+}]_{cyt}^p}{K_{SERCA}^p+[Ca^{2+}]_{cyt}^p}, \tag{9}$$

$$J_{PMCA}=V_{PMCA}\frac{[Ca^{2+}]_{cyt}^q}{K_{PMCA}^q+[Ca^{2+}]_{cyt}^q}. \tag{10}$$

2.3. CRAC channel model

STIM1 was identified through RNAi screens and soon proved to be the ER Ca^{2+} sensor [26–29]. Experiments show that a STIM1-horseradish peroxidase fusion protein accumulates within junctional ER structures located 10–25 nm from the plasma membrane. Although the relocation of STIM1 into junctional ER region is slow [29], it is indeed prior to the activation of I_{CRAC} by 0–20 s, with an average of 6–10 s [42]. Mutations in EF-hand of STIM1 reduce its affinity to Ca^{2+}, and hence mimicking the store-depleted state, activate I_{CRAC} even when the Ca^{2+} store is full [28,29,35]. The recombinant EF-SAM fragment readily tends to form the dimer in the absence of Ca^{2+} ions [43].

Orai1 is a plasma membrane protein with four-transmembrane domains and intracellular N and C termini. Mutagenesis of acidic residues reduces the divalent and monovalent selectivity of I_{CRAC}, and these studies offer definitive evidence that Orai1 is a subunit of the CRAC channel. It seems likely that the native CRAC channel is either an Orai1 homomultimer alone or a heteromultimer with Orai2 and /or Orai3 [34,36,44].

In the present work, we suppose that two Ca^{2+} ions cooperatively dissociate from the EF-hands of the STIM1 dimers (and/or oligomers) in ER membrane. The apoSTIM1 dimers (and/or oligomers) need to be activated before they bind to the CRAC channels. Then, the active dimers are readily to trigger the activation of CRAC channels. The dissociation kinetics of Ca^{2+} can be expressed by Eqs. (11) and (12). In addition, we simplify the dissociation process by fixing the Hill coefficient to 2 in Eq. (11). It should be noted that attempts to confirm the true kinetic mechanisms of STIM1 activation and oligomerization are still under way.

$$[S_2]=\frac{K_1^2}{[Ca^{2+}]_{ER}^2+K_1^2}([S_T]-[S_{2a}]), \tag{11}$$

$$\frac{d[S_{2a}]}{dt}=k_a[S_2]-k_i[S_{2a}], \tag{12}$$

$$\frac{d[S_4]}{dt}=V_{S_4}\frac{[S_2]^2}{[S_2]^2+K_2^2}-k_d[S_4]. \tag{13}$$

Where, S_2 is the Ca^{2+} apoSTIM1 dimer, S_{2a} is the activated apoSTIM1 dimer, and S_4 is the apoSTIM1 tetramer and/or higher oligomer. K_1 is the apparent dissociation constant of ER Ca^{2+} to STIM1 dimers. K_2 is the apparent dissociation constant for oligomers. The Hill coefficient 2 in Eq. (13) absolutely stands for at least two dimers interacting with each other to form a tetramer or a higher oligomer. But to our knowledge, it seems to be difficult to provide an accurate stoichiometric relationship for the cooperative oligomerization of STIM1 dimers at present.

Orai1 is thought to be an essential pore subunit for Ca^{2+} channels in plasma membrane in T cells. Although the phenomenon of store-operated Ca^{2+} entry was first described decades ago, the detailed mechanisms linking the depletion of ER Ca^{2+} to the activation of CRAC channels still remain unidentified. In this work, we suppose that four Orai1 subunits assemble a multimeric CRAC channel.

The dynamic equations expressing the assembly, disassembly and activation of CRAC channels can be written as follows:

$$\frac{d[O]_c}{dt}=V_{cp}\frac{[Orai1]^n}{K_c^n+[Orai1]^n}-k_{dc}[O]_c-k_{op}\frac{[S_{2a}]^l[O]_c}{K_o^l+[S_{2a}]^l}+k_{od}[O]_o, \tag{14}$$

$$\frac{d[O]_o}{dt} = k_{op}\frac{[S_{2a}]^l[O]_c}{K_o^l + [S_{2a}]^l} - (k_{od} + k_{do})[O]_o, \quad (15)$$

Where, $[O]_c$ represents the concentration of closed CRAC channels which disallows the Ca^{2+} flow across the plasma membrane. n is the Hill coefficient representing the cooperative interactions in Orai1 subunits. $[O]_o$ is the concentration of opened CRAC channels which is active and responsible for Ca^{2+} entry. We suggest that the activation of opened CRAC channels is subject to the interactions between activated apoSTIM1 dimers (and/or higher oligomers) and the closed channels.

Assuming the concentration of total Orai1 subunits keeps constant, we obtain

$$[\text{Orai1}]_{\text{total}} = [\text{Orai1}] + r([O]_c + [O]_o), \quad (16)$$

Thus, the total influx through the plasma membrane is given by the following equation,

$$J_{\text{PMchannel}} = (k_{soc}[O]_o + V_{\text{PMleak}})\left([Ca^{2+}]_{ec} - [Ca^{2+}]_{cyt}\right). \quad (17)$$

Here, k_{soc} is the rate constant of Ca^{2+} entry through CRAC channels, and V_{PMleak} is the leak of Ca^{2+} from extracellular pool to cytoplasm.

3. Results

3.1. Ca^{2+} oscillations in ER and cytoplasm

The numerical simulation of Ca^{2+} oscillations is shown in Fig. 1. All the parameters and constants are taken the values in Table 1 except for $n=3$ and $r=4$, respectively.

Under these conditions, the $[Ca^{2+}]_{cyt}$ shows a sustained oscillation, with a period of 29.1 s and amplitude of ~1.48 μM [Fig. 1(a)]. $[Ca^{2+}]_{ER}$ shows a different oscillation profile from $[Ca^{2+}]_{cyt}$ as the refilling of ER Ca^{2+} undergoes two distinguishable phases, a fast and a slow phases respectively. The turning point is at ~6.8 μM of $[Ca^{2+}]_{ER}$ (Fig. 1(b)). In Fig. 1(a) and (b), we find that the fast phase of ER Ca^{2+} refilling is exactly corresponding to the time course of the cytoplasmic Ca^{2+} pulse. Generally, the ER Ca^{2+} flux consists of three main parts: a leak and a flux of IP_3R Ca^{2+} channel, those two outward ER; and an inward flux via SERCA (Eq. (2)). At maximum $[Ca^{2+}]_{cyt}$ (~1.48 μM), SERCA Ca^{2+} pump reaches its maximum rate at 0.99 V_{SERCA} in our model owing to its cooperative characteristics (parameters taken from Table 1). In the absence of cooperativity, the maximum rate is only ~0.91 V_{SERCA}. It is of evidence that a cooperative SERCA pump allows a rapid uptake of the cytoplasmic Ca^{2+} back to the ER. For example, a totally delayed clearance of the cytoplasmic Ca^{2+} is generally observed without the cooperativity of SERCA pump [21]. The PMCA Ca^{2+} pump plays a two-edged role in the cytoplasmic Ca^{2+} oscillation. On the one hand, it accelerates the clearance of the cytoplasmic Ca^{2+} and results in the fast refilling of ER Ca^{2+} in combination with SERCA pump. On the other hand, PMCA causes the significant loss of Ca^{2+} in cytoplasm, which finally prolongs the refilling time to the maximum $[Ca^{2+}]_{ER}$ and leads to a slow refilling of ER Ca^{2+}.

In Fig. 1(c), we observe that the $[Ca^{2+}]_{cyt}$ only changes little as the $[Ca^{2+}]_{ER}$ increases from ~6.8 μM to its maximum concentration. Therefore, the fast clearance of the cytoplasmic Ca^{2+} is nearly done at this $[Ca^{2+}]_{ER}$ (~6.8 μM) while the refilling of ER Ca^{2+} still remain approximately 50% to be finished. It is of interest that a slow Ca^{2+} augmentation in cytoplasm is correlated with the left 50% of ER Ca^{2+} refilling. In fact, when the $[Ca^{2+}]_{ER} > 6.8$ μM, the Ca^{2+} net influx toward cytoplasm is only slightly greater than the net efflux. It leads to a very slow increase of $[Ca^{2+}]_{cyt}$. Meanwhile, the opened CRAC channels continue to mediate the Ca^{2+} influx in plasma membrane, which further forces the $[Ca^{2+}]_{ER}$ to its maximum via SERCA Ca^{2+} pump. If the Ca^{2+} influx through the CRAC channels is controllable, the time for the slow phase of ER Ca^{2+} refill will be easily regulated. Then the period of

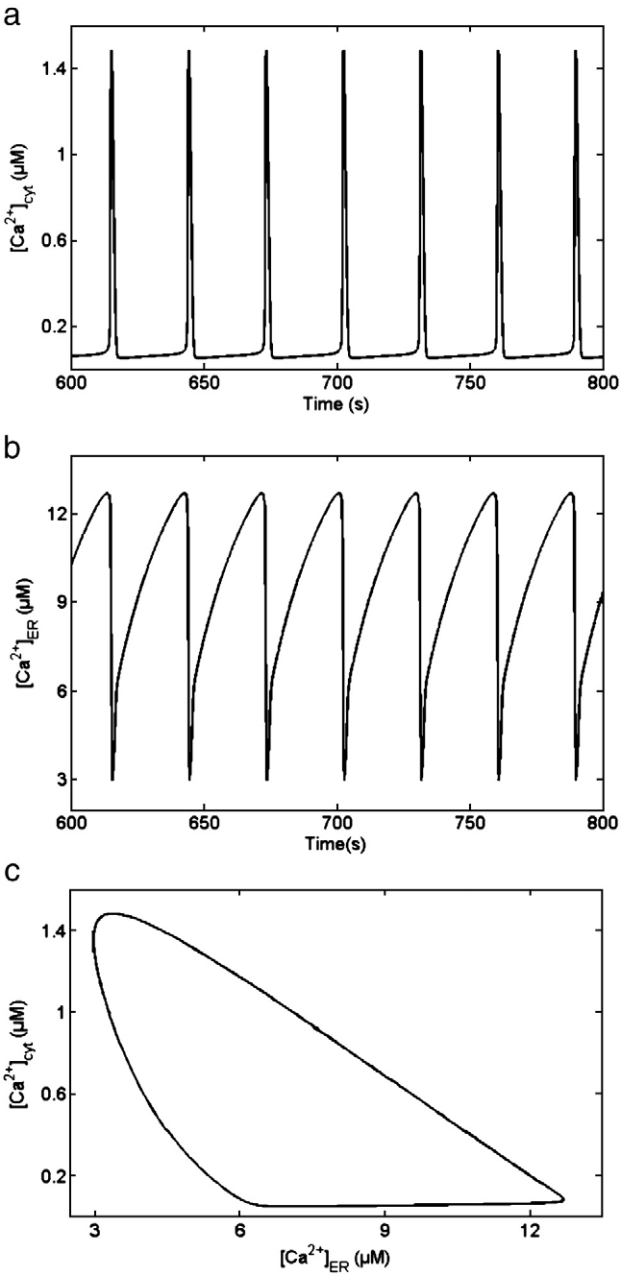

Fig. 1. Numerical simulation of $[Ca^{2+}]_{cyt}$ and $[Ca^{2+}]_{ER}$ oscillations in a T cell. (a) $[Ca^{2+}]_{cyt}$ oscillation. The period is 29.1 s. The amplitude is 1.48 μM. (b) $[Ca^{2+}]_{ER}$ oscillation. The minima and maxima are 2.97 and 12.7 μM, respectively. (c) Phase plot of $[Ca^{2+}]_{cyt}$ versus $[Ca^{2+}]_{ER}$.

Ca^{2+} oscillation is readily adjusted according to the Ca^{2+} influx in plasma membrane. We conclude that a cooperative CRAC channel plays a crucial role in the second part of ER Ca^{2+} refilling. The differences of a non-cooperative CRAC channel in the Ca^{2+} oscillation will be discussed in detail (in Section 3.3).

3.2. Activation, dimerization and /or oligomerization of apoSTIM1

The activity of STIM1 depends on the $[Ca^{2+}]_{ER}$. Upon depletion of ER Ca^{2+}, the apoSTIM1 readily tends to dimerize and/or oligomerize [32]. Fig. 2(a) shows the saturation kinetics of the activated STIM1 dimers (S_{2a}). S_{2a} is the active form triggering the opening of the CRAC channels in plasma membrane. To our knowledge, the mechanisms about STIM1 activation and the formation of dimer have not been

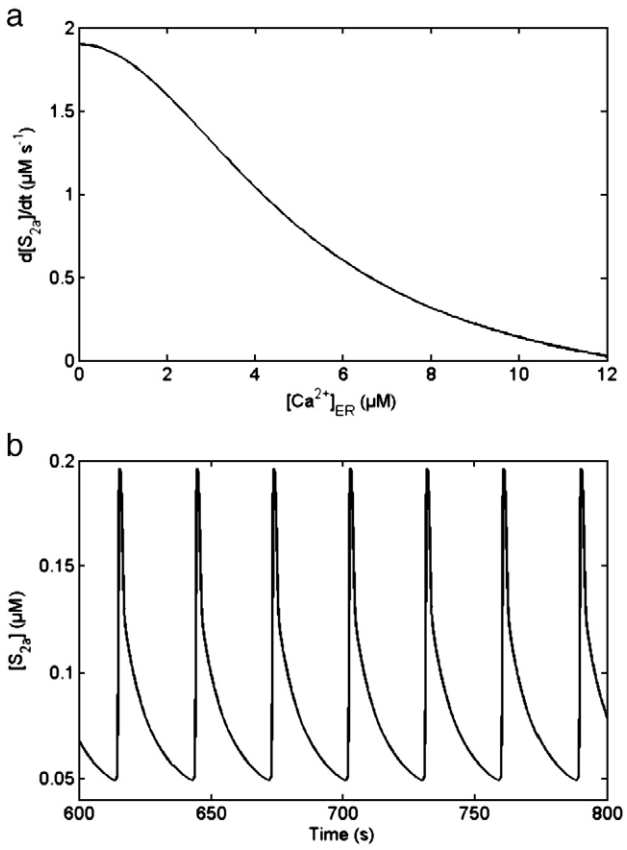

Fig. 2. Sigmoid saturation behavior of apoSTIM1 dimers. (a) Plot of apoSTIM1 dimer versus $[Ca^{2+}]_{ER}$ (Eq. (12)). (b) Oscillation profile of $[S_{2a}]$.

made clear till now. In this paper, we assume that the dissociation of Ca^{2+} from STIM1 has following reactions.

$$SCa^{2+} + SCa^{2+} \rightleftharpoons [SCa^{2+}]_2, \tag{18}$$

$$[SCa^{2+}]_2 \rightleftharpoons [S]_2 + 2Ca^{2+}. \tag{19}$$

Where, $\underline{[SCa^{2+}]_2}$ and $\underline{[S]_2}$ are the STIM1 dimer and apoSTIM1 dimer, respectively. We deal with Eq. (18) as a simple equilibrium reaction while Eq. (19) has a strong cooperativity in Ca^{2+} dissociation kinetics.

For simplicity, we omit the calculation of the concentration of STIM1 monomer and assume the total quantity of STIM1 dimers to be a constant. Then we obtain Eq. (11) representing for the dissociation kinetics of the Ca^{2+} in STIM1 dimers. The concentration of the activated apoSTIM1 dimer is given in Fig. 2(a). As to higher oligomers, we use S_4 in Eq. (13) for active apoSTIM1 instead of S_{2a} in Eq. (12). However, the results show no significant change, thus we only discuss the effect of apoSTIM1 dimers on the activation of CRAC channels regardless of the higher oligomers. The oscillation dynamics of the activated apoSTIM1 dimer is shown in Fig. 2(b). A steep pulse is observed before the $[Ca^{2+}]_{ER}$ decreases to ~1.2 μM. Such fast activation of STIM1and deactivation of apoSTIM1 processes result from the calcium-induced calcium release via IP_3R [5,6] and the rapid refilling of ER Ca^{2+}.

3.3. Effects of CRAC channels' cooperativity and k_{soc} on Ca^{2+} oscillation

The cooperativity is ubiquitous in living cells. In most cases, the oscillation dynamics are directly or indirectly controlled by the cooperative interactions. In this paper, we analyze the Ca^{2+} entry via the non-cooperative and the cooperative CRAC channels, respectively (Fig. 3). In Fig. 3(a), there is no cooperativity in monomer channel

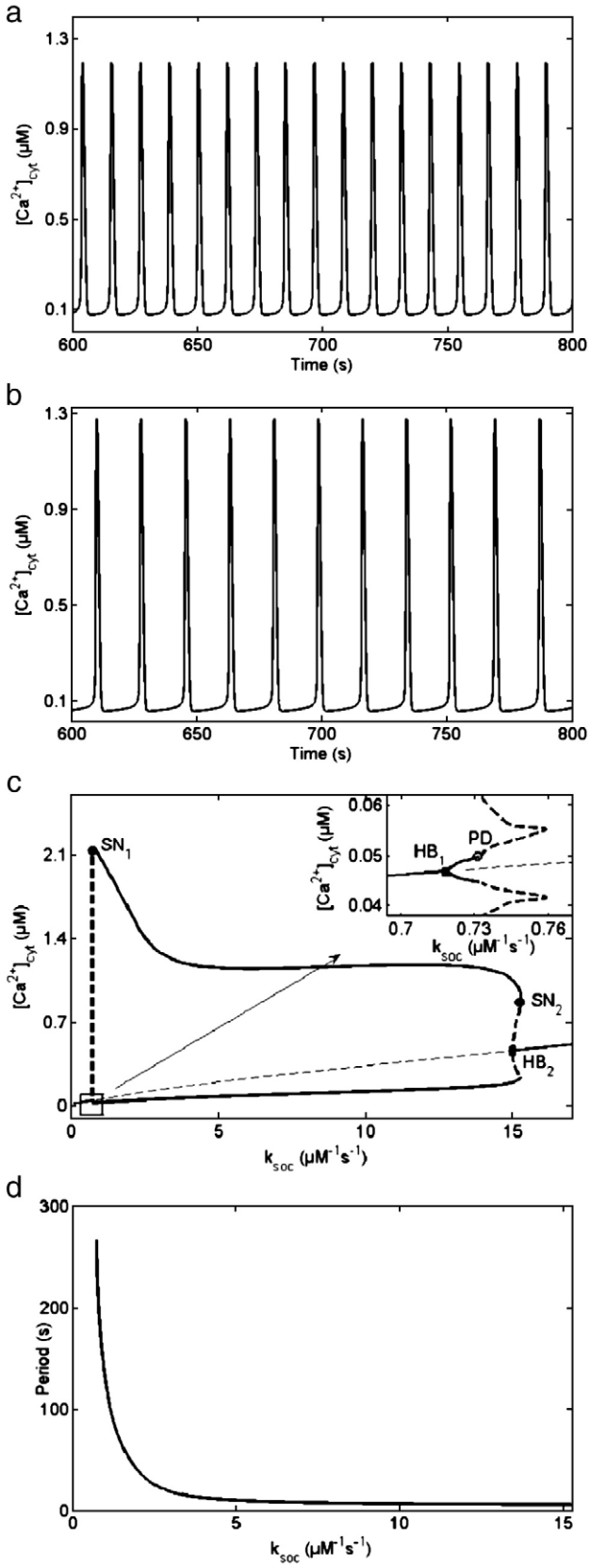

Fig. 3. Effects of CRAC channels' cooperativity changes on $[Ca^{2+}]_{cyt}$ oscillation. (a) $n=1$, $r=1$. Period, 11.6 s. (b) $n=2$, $r=3$. Period, 17.7 s. For $n=3$, $r=4$, see Fig. 1(a), (c) Bifurcation diagram of $[Ca^{2+}]_{cyt}$ as a function of k_{soc}. HB, PD, SN represent the Hopf bifurcation, period-doubling bifurcation and Saddle-node bifurcation, respectively. (d) Plot of the period versus k_{soc}. For frequency encoding signal, the effective values of k_{soc} is from ~0.723 to ~2.78 $\mu M^{-1}\ s^{-1}$.

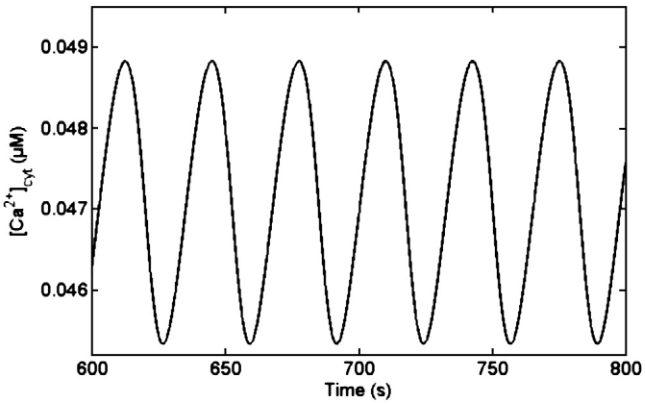

Fig. 4. Dynamic simulation of stable $[Ca^{2+}]_{cyt}$ oscillation between the HB_1 and PD. Where, k_{soc}=0.725 μM^{-1} s^{-1}. The period is 32.3 s.

assembly (n=1, r=1). The $[Ca^{2+}]_{cyt}$ oscillation has the period of 11.6 s and the amplitude of 1.19 μM. In contrast, a previous study shows that a linear CRAC channel model (without cooperativity) usually causes no oscillation or a prolonged period of Ca^{2+} oscillation in order to get the ideal amplitude [21]. When n=2, and r=3, the period and the amplitude become 17.7 s and 1.28 μM, respectively (Fig. 3(b)). In addition, we compare the Ca^{2+} oscillation behavior shown in Fig. 1(a), where n=3, and r=4. Due to the cooperativity changes in CRAC channels assembly, it is noticeable that the period increases significantly by 2.51 times to 29.1 s but the Ca^{2+} oscillation amplitude only increases by 1.24 times to 1.48 μM. Rooney et al. observed in experiments that the periods of $[Ca^{2+}]_{cyt}$ oscillates in a wide range from >250 s for low hormone doses, to ~30 s for higher hormone concentrations [33]. Höfer et al. have demonstrated previously that a coupled IP_3–Ca^{2+} oscillator had a very similar dynamic behavior, the frequency (or the period) is more sensitive than the amplitude to the changes of dynamic parameters [4]. This frequency-modulated Ca^{2+} oscillation in cytoplasm may have vital functions in living cell as the Ca^{2+} hemostasis is critical for the physiological activities. A very high concentration of the cytoplasmic Ca^{2+} is toxic and definitely results in cell death. It restricts the fluctuation of $[Ca^{2+}]_{cyt}$ only in a narrow range. As a result, although the amplitude of Ca^{2+} may be responsible for some information exchanges in living cells [34,35], the frequency of Ca^{2+} oscillation appears to be the more effective candidate available for signal encoding.

The bifurcation diagram is indicated in Fig. 3(c). The solid and dashed lines represent stable and unstable states, respectively. For small values of k_{soc}, $[Ca^{2+}]_{cyt}$ is in a single stable steady-state.

When k_{soc}>0.72 μM^{-1} s^{-1}, the system shifts from the stable steady-state to a stable oscillation in the first Hopf bifurcation (HB_1). This stable oscillation is limited in a narrow region of k_{soc} values, from 0.72 to 0.733 μM^{-1} s^{-1} (Fig. 5). For k_{soc}>0.733 μM^{-1} s^{-1}, the system becomes unstable in a period-doubling bifurcation (PD).

Crossing the first saddle-node (k_{soc}=0.724 μM^{-1} s^{-1}, $[Ca^{2+}]_{cyt}$= 2.14 μM), the cytoplasmic Ca^{2+} remains in a stable oscillation before reaching the second saddle-node (k_{soc}=15.3 μM^{-1} s^{-1}, $[Ca^{2+}]_{cyt}$= 0.853 μM). SN_1 and SN_2 represent the two saddle-nodes, respectively. The Ca^{2+} oscillation is not stable between the second saddle node (SN_2) and the second Hopf bifurcation (HB_2) where k_{soc}=15 μM^{-1} s^{-1}. For k_{soc}>15 μM^{-1} s^{-1}, the system returns to a stable steady-state. Fig. 3(d) shows the period of the $[Ca^{2+}]_{cyt}$ oscillation as a function k_{soc}. One notices that the period monotonically decreases as the k_{soc} value increases. In our frequency-modulated system, the effective k_{soc} values may range from ~0.73 to ~15 μM^{-1} s^{-1} for the cytoplasmic Ca^{2+} signal encoding.

Researchers have previously showed that the devoid of SOC channels' function causes no Ca^{2+} oscillation in cytoplasm [17]. Thus, we assign a trivial Ca^{2+} leak in plasma membrane in resting state. It abolishes the Ca^{2+} oscillation in the absence of CRAC channels. When k_{soc}<0.720 μM^{-1} s^{-1}, Ca^{2+} influx in plasma membrane is too small to trigger the IP_3R Ca^{2+} channel to open effectively. The system is in a stable steady-state. From the HB_1 to the PD point, the IP_3R Ca^{2+} channel is still inactivated but the Ca^{2+} influx rate (toward cytoplasm) slightly exceeds the clearance rates of the SERCA and PMCA pumps at the beginning (Fig. 4). At the maximum $[Ca^{2+}]_{cyt}$, the SERCA and PMCA clearance rate increases to ~0.0957 and ~0.0116 μM s^{-1}, respectively. The pump clearance rates now surpass the Ca^{2+} influx rate, and the Ca^{2+} is removed from cytoplasm. Under these conditions, we only observe very small amplitude of Ca^{2+} oscillation. Between HB_1 and PD, the IP_3R Ca^{2+} channel is activated and begins to open gradually and slightly. The influx and the clearance of the cytoplasmic Ca^{2+} establish a subtle equilibrium, which is liable to be perturbed by the small variations of the Ca^{2+} influx and/or efflux rates (Fig. 3(c)). We have known nothing about the biological significance of this oscillation behavior of the cytoplasmic Ca^{2+}.

From SN_1 to SN_2, the IP_3R Ca^{2+} channel is fully activated. Meanwhile, a solid equilibrium is established between the Ca^{2+} influx and efflux in cytoplasm. Between SN_2 and HB_2, the Ca^{2+} oscillation begins to be inhibited. Crossing HB_2, the Ca^{2+} oscillation is fully inhibited. Two reasons may be responsible for this dynamic change: one is the inactivation of IP_3R Ca^{2+} channel at higher cytoplasmic Ca^{2+}; the other is the decrease of IP_3 production mediated via feedback control, which we will discuss later (see Eq. (7) in details).

We investigate the dynamic behavior of the opened CRAC channels in the presence of cooperativity (Fig. 5). The peak value of opened CRAC channels has a ratio of ~12% to the total concentration of Orai1 monomers. It is interesting that the CRAC channels constantly has a high fraction opened at the resting state, a ratio of ~5.6% to the total Orai1 concentration. We deduce that a permanent Ca^{2+} leak in plasma membrane is mostly attributed to the opened CRAC channels at its resting state. The Ca^{2+} leak through other pathways is definitely trivial.

We also study the oscillation profile of the opened CRAC channels for n=1, r=1 and n=2, r=3, respectively (Fig. 4). Compared the result with the Fig. 5, it is concluded that the cooperatively assembled and activated CRAC channels play a key role in regulating the period of Ca^{2+} oscillation (Table 2). In Table 2, all the channel concentrations are the average values expressed in Eq. (20).

$$\overline{[O]}_i = \frac{1}{T}\int_0^T [O]_i(t)\mathrm{d}t. \tag{20}$$

Where, $[O]_i(t)$ represents the concentration of $[O]_c$ or $[O]_o$ at time t. In fact, a highly cooperative CRAC channel adequately controls two

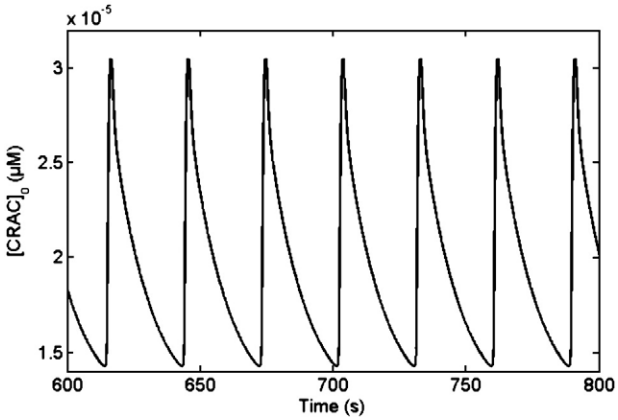

Fig. 5. Oscillation dynamics of opened CRAC channels. The parameters and constants are taken in Table 1 except for n=3, and r=4.

Table 2
The effect of the cooperativity on the cytoplasmic Ca^{2+} oscillation and the quantities of CRAC channels

	$n=1$	$n=2$	$n=3$
	$r=1$	$r=3$	$r=4$
$\frac{[O]_{io}+[O]_{ic}}{[Orai1]_{total}}$	0.47	0.323	0.244
$\frac{[O]_{io}}{[O]_{io}+[O]_{ic}}$	0.092	0.0875	0.0786
Period (s)	11.6	17.7	29.1
Amplitude (μM)	1.19	1.28	1.48

critical factors, the total quantity of the channels and the quantity of the active channels. In the absence of cooperativity ($n=1$, $r=1$), the period of Ca^{2+} oscillation is probably too short compared with the period in physiological situations [33]. A trimeric CRAC channel ($n=2$, $r=3$) has a period of 17.7 s which is still beyond the normal range of the Ca^{2+} oscillation period. The tetrameric channel allows a suitable period with a slight increase in amplitude. We infer that a high cooperativity in the self-assembled CRAC channel may be one of the most efficient factors to modulate the Ca^{2+} oscillation period in T cells.

3.4. Feedback effect of cytoplasmic Ca^{2+} on IP_3 production

IP_3 plays an essential role in regulating the cytoplasmic Ca^{2+} oscillation. In this work, we study the IP_3 dynamics with the modified feedback pathways to clarify the effect of IP_3. The bifurcation diagrams of our mixed feedback model are compared with the single negative and positive feedback model as a function of V_{PLC}, (Fig. 6(a) and (c)), and a function of k_{deg} (Fig. 6(b) and (d)), respectively.

When $K_{PLC}=0$, the cytoplasmic Ca^{2+} has a negative feedback regulation on IP_3 production (Fig. 6(a)). A stable Ca^{2+} oscillation is observed between the first Hopf bifurcation ($V_{PLC}=0.0635$ μM s^{-1}), represents by HB_1, and the first period-doubling bifurcation ($V_{PLC}=0.0770$ μM s^{-1}), represents by PD_1. For $V_{PLC}>0.0770$ μM s^{-1}, the system becomes unstable until the second period-doubling bifurcation (PD_2), where $V_{PLC}=0.198$ μM s^{-1}. For $V_{PLC}>0.198$ μM s^{-1}, the system returns to the stable oscillation with the high frequency and large amplitude. Then, passing through the second Hopf bifurcation (HB_2) point, the system becomes a single stable steady-state.

In Fig. 6(b), when $K_{deg}=0$, it stands for a positive feedback effect of Ca^{2+} on IP_3 production. The bifurcation dynamics is relatively simple since only one Hopf bifurcation point ($k_{deg}=0.0413$ s^{-1}) is observed throughout the full range of k_{deg} values we investigate. The dynamic system shows a stable Ca^{2+} oscillation provided $k_{deg}<0.146$ s^{-1}. It is important to notice that, in negative feedback inhibition, an increase in V_{PLC} value causes a decrease in the amplitude of the cytoplasmic Ca^{2+} oscillation in contrast to the positive feedback regulation in Fig. 6(b), where the greater k_{deg} values lead to the larger Ca^{2+} oscillation amplitudes.

In the mixed feedback model ($K_{PLC}\neq0$, and $K_{deg}\neq0$), the bifurcation dynamics are analyzed through a fixed value of V_{PLC} or k_{deg} (Fig. 6(c) and (d)). Although this method cannot represent a global dynamic behavior for the mixed feedback model, some differences are still observed. Compared with a single positive feedback model, the mixed model has a more proper range of the Ca^{2+} amplitude (Fig. 6(c)). In addition, the mixed model allows a stable, and sustained cytoplasmic Ca^{2+} oscillation at a wider range of k_{deg} values. However, a single positive feedback model shows a stable oscillation only at narrow range of k_{deg}. When both n and r are equal to 1, the simulation results of the feedback effect of cytoplasmic Ca^{2+} on IP_3 production are similar to Fig. 6(c) and (d), except that the amplitude of Ca^{2+} oscillation and the ranges of V_{PLC} and k_{deg} for stable oscillation have little distinctions (data not shown).

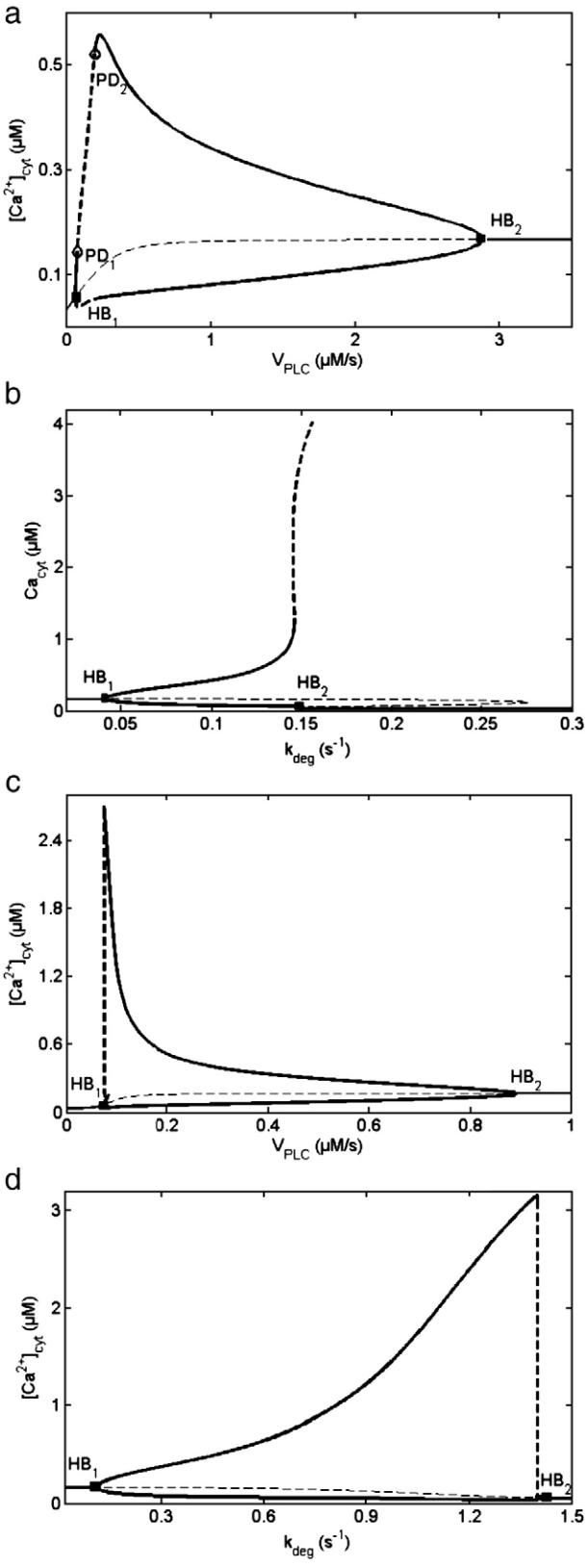

Fig. 6. Feedback effect of $[Ca^{2+}]_{cyt}$ on IP_3 production. Bifurcation diagrams of $[Ca^{2+}]_{cyt}$ are calculated as a function of V_{PLC} (Fig. 6(a) and (c)), and a function of k_{deg} (Fig. 6(b) and (d)). The solid and dashed lines stand for stable and unstable states, respectively. (a) $K_{PLC}=0$. Two HB points at $V_{PLC}=0.0635$ and 2.88 μM s^{-1}. Two PD points, $V_{PLC}=0.077$ and ~0.198 μM s^{-1}. (b) $K_{deg}=0$. Two HB point at $k_{deg}=0.0413$ s^{-1} and $k_{deg}=0.148$ s^{-1}. (c) $K_{PLC}=0.12$, and $K_{deg}=0.1$. $k_{deg}=0.1$ s^{-1}. Two HB points at $V_{PLC}=0.0714$ and 0.891 μM s^{-1}. Two PD points at $V_{PLC}=0.075$ and 0.0758 μM s^{-1} (d) $V_{PLC}=1.0$ μM s^{-1}. Other parameters and constants are the same as in Fig. 6(c). Two HB points at $k_{deg}=0.112$ and 1.44 s^{-1}. Two SN points at $k_{deg}=1.391$ and 1.396 μM s^{-1}.

4. Discussion

STIM1 and Orai1 play critical roles in the sustained Ca^{2+} entry, and thus regulate the gene expressions in T cells. These two proteins also account for a considerable portion of SOCE in some other cells [17]. Severe combined immunodeficiency (SCID) is a rare inherited disease, and the T lymphocytes from patients completely lack I_{CRAC} and cannot be activated by physiological signals. The genetic mapping reveals that SCID is caused by a R91W point mutation in Orai1 [46]. Although growing evidence supports that SOCs functions in the maintenance of cytoplasmic Ca^{2+} oscillation, some details about SOCs are still unidentified. One is whether Orai1 gene stands for all SOCs. It is noticeable that distinct SOCs exist in different types of cells. For example, in EBV-transformed B cells, the R91W mutant Orai1 only partially reduces its Ca^{2+} influx, but the SOCE is totally eliminated in human T cells [31]. Another unanswered question is whether there is different Ca^{2+} entry mechanism existed in non-excitable cells. Electrophysiological studies have demonstrated that membrane currents have diverse properties in different cells upon depletion of ER Ca^{2+}, illustrating different types of cells might have their own specific SOCs. The superfamily of transient receptor potential (TRP) channels has been investigated as the candidates for over a decade. However, the results indicate under certain conditions some TRP channels (TRPs) may form, or be part of SOCs, the functions of TRPs as SOCs are still unknown [2]. One report confirms that a ternary complex TRPC1/STIM1/Orai1 is formed in response to the internal Ca^{2+} depletion [47]. In fact, it is difficult to verify that whether TRPs are activated by depletion of ER Ca^{2+} or by other signals that coincide with store depletion. Additionally, one possibility is still under debate that SOCE is generally responsible for the restoration of ER Ca^{2+} after intense stimuli and the Ca^{2+} for intracellular signaling under normal physiological stimulations is mostly via non-store-operated channels [48].

In many cell types, the oscillation of cytoplasmic Ca^{2+} are eliminated when Ca^{2+} is removed from the extracellular environment, suggesting that there is a definitive relationship between Ca^{2+} entry in plasma membrane and the cytoplasmic Ca^{2+} oscillation [49–52]. As mentioned above, other works have shown that some types of TRPs are responsible for the maintenance of Ca^{2+} oscillation [53,54].

Owing to the structural complexities and functional diversities of non-excitable cells, there is no general model suitable for different cell types in SOCE-dependent Ca^{2+} oscillation. At present, whether SOCs plays a specific role in cytoplasmic Ca^{2+} oscillation at submaximal agonist concentrations or under a modest depletion of stores is still disputable. In this work, we propose a simple model to mimic the Ca^{2+} dynamics in cytoplasm based on the recent findings in STIM1 and Orai1. The application of our model should be limited only to some types of non-excitable cells dependent on SOCs such as T cells. Further, the activation of Orai1 CRAC channel in our model depends on the ER Ca^{2+} depletion. The situation is closely related to a series of continuing stimuli under physiological circumstances or the intense stimuli in pharmacological conditions such as high doses of agonists.

We try to set up a linking among the ER Ca^{2+}, the STIM1 protein, the CRAC channel and the cytoplasmic Ca^{2+} through a theoretical model. Our model is built on three assumptions: (1) Ca^{2+} cooperatively dissociates from the STIM1 dimers upon reduction of the ER luminal Ca^{2+}; (2) the Orai1 monomers spontaneously tend to form an inactive and multimeric (most probably a tetrameric) CRAC channel; (3) the apoSTIM1 (Ca^{2+} unbound STIM1) dimers trigger the activation of CRAC channels, the activated channels then mediate the Ca^{2+} entry in plasma membrane. In addition, we assume that the cytoplasmic Ca^{2+} has a mixed feedback (including a negative and a positive feedback loops) effect on IP_3 production. Therefore, we obtain a set of nonlinear differential equations to describe the effect of CRAC channel on the Ca^{2+} entry in plasma membrane and the Ca^{2+} oscillation in cytoplasm. Using our proposed kinetic equations, and combined with the modified Li–Rinzel model, we can quantitatively analyze the processes of the activation of STIM1, and the assembly, disassembly and activation of Orai1 CRAC channels. The characteristics of frequency-modulated [4] of Ca^{2+} oscillation still hold true in our model.

A low sustained Ca^{2+} influx is constantly observed in our model through Orai1 CRAC channels. In Table 2, it shows that only a small portion of CRAC channels (about 7.9%) is activated upon depletion of ER Ca^{2+}. Experiments demonstrate that each low-conductance CRAC channel transports ~10^4 Ca^{2+} ions per second. In contrast, a high-conductance L-type Ca^{2+} channel, which triggers a fast burst release of insulin from pancreatic β cells, delivers ~5×10^5 Ca^{2+} ions in one second [17,55]. Hogan and Rao deduce that the low-conductance CRAC channel may have two functions. If active CRAC channels form clusters at plasma-membrane–ER-membrane junctions, it seems that the small current via each opened channel effectively controls the possibly large fluctuations in the concentrations of cytoplasmic Ca^{2+} within the restricted space between the apposed membranes. In addition, if CRAC channels transport Ca^{2+} directly into a relatively less-restricted space, the small current may guarantee small changes in local Ca^{2+} concentration near the channel [17]. We suggest that the low sustained Ca^{2+} influx is attributed to a small population of apoSTIM1 dimers which are cooperatively regulated by ER Ca^{2+} and then trigger the activation of closed CRAC channels.

To test the compatibility of our CRAC model, we have also combined it with the electrochemical model proposed by Marhl et al. [14] in an open cell system. All the parameters were taken from Table 1 or within the range of the values used in Reference [14], the joint model shows the very closed dynamic profiles in cytoplasmic and ER Ca^{2+} oscillations compared with the original model except for the modifications of V_{PMCA} and K_1 in our model (a decrease in V_{PMCA} to 0.24 $\mu M^{-1}\ s^{-1}$ and an increase in K_1 to 50 μM). In addition, the period and the amplitude of open CRAC channels in De Young–Keizer–Li–Rinzel model are 29.1 s and 1.6×10^{-5} μM, while those in the model by Marhl et al. are 30 s and 2.9×10^{-5} μM, respectively. Therefore, it is proved that our CRAC model can be extended to other Ca^{2+} dynamic model as a plug-in unit. Definitely, the validity of the CRAC model for other types of Ca^{2+} dynamic models is still unknown. For clarity, simulation data have not been presented here.

In the present work, we suggest that a tetrameric Orai1 CRAC channel can effectively control the total quantity of CRAC and the quantity of active CRAC channel, which finally affects the period and amplitude of cytoplasmic Ca^{2+} oscillation. Our results agree well with published experimental data. We find that a constant leak of Ca^{2+} in plasma membrane is mostly due to the Ca^{2+} influx through a fraction of opened Orai1 CRAC channels. In the absence of cooperativity in the STIM1 activation (The Hill coefficient equals to 1 in Eq. (11)), we obtain a less amplitude and a shorter period of STIM1 compared with the results in Fig. 3(b) (data not shown). In addition, our mixed feedback assumption of the cytoplasmic Ca^{2+} on IP_3 production may extend the range of some parameters' values, for example k_{deg}, and allow the suitable Ca^{2+} amplitudes in T cells.

IP_3 oscillation is not essential for a sustained Ca^{2+} oscillation in the cells [16,56–59] according to the models proposed in all literatures provided that the Ca^{2+}-induced Ca^{2+} release (CICR) or any other Ca^{2+} autocatalytic release mechanism is introduced. But, IP_3 dynamic behaviors really have a significant effect on the range of parameter values and the oscillation patterns for Ca^{2+} oscillation in hepatocytes [60]. An inhibition of protein kinase C in hamster ovary eggs eliminates the Ca^{2+} oscillation while IP_3 formation is still maintained [61]. In many cases, a fixed IP_3 value makes the theoretical model more concisely without loss of the dynamic system's generality and validity. A variable IP_3 used in our work may offer us some extra information about the complex impact of IP_3 on Ca^{2+} oscillations in non-excitable cells. Certainly, the detailed dynamic analyses of our mixed model need to survey the full range of V_{PLC} and k_{deg} values related to the cytoplasmic Ca^{2+} oscillations. In addition, the other types of SOCs and the non-store-operated channels need to be included in our future work. A more applicable model incorporated with new achievements is to be expected.

References

[1] J.S. Marchant, Cellular signalling: STIMulating calcium entry, Curr. Biol. 15 (2005) R493–R495.
[2] J.T. Smyth, W.I. Dehaven, B.F. Jones, J.C. Mercer, M. Trebak, G. Vazquez, J.W. Putney Jr., Emerging perspectives in store-operated Ca^{2+} entry: roles of Orai, Stim and TRP, Biochim. Biophys. Acta 1763 (2006) 1147–1160.
[3] A. Rozi, Y. Jia, A theoretical study of effects of cytosolic Ca^{2+} oscillations on activation of glycogen phosphorylase, Biophys. Chem. 106 (2003) 193–202.
[4] A. Politi, L.D. Gaspers, A.P. Tomas, T. Höfer, Models of IP_3 and Ca^{2+} oscillations: frequency encoding and identification of underlying feedbacks, Biophys. J. 90 (2006) 3120–3133.
[5] G.W. De Young, J. Keizer, A single-pool inositol 1,4,5-trisphosphate-receptor-based model for agonist-stimulated oscillations in Ca^{2+} concentration, Proc. Natl. Acad. Sci. U. S. A. 89 (1992) 9895–9899.
[6] Y.X. Li, J. Rinzel, Equations for $InsP_3$ receptor-mediated $[Ca^{2+}]_i$ oscillations derived from a detailed kinetic: a Hodgkin–Huxley like formalism, J. Theor. Biol. 166 (1994) 461–473.
[7] I. Bezprozvanny, J. Watras, B.E. Ehrlich, Bell-shaped calcium response curves of Ins (1,4,5)P_3- and calcium-gated channels from endoplasmic reticulum of cerebellum, Nature, 351 (1991) 751–754.
[8] T. Meyer, L. Stryer, Molecular model for receptor-stimulated calcium spiking, Proc. Natl. Acad. Sci. U. S. A. 85 (1988) 5051–5055.
[9] A. Goldbetter, G. Dupont, M.J. Berridge, Minimal model for signal-induced Ca^{2+} oscillations and for their frequency encoding through protein phosphorylation, Proc. Natl. Acad. Sci. U. S. A. 87 (1990) 1461–1465.
[10] R. Somogyi, J.W. Stucki, Hormone-induced calcium oscillations in liver cells can be explained by a simple one pool model, J. Biol. Chem. 266 (1991) 11068–11077.
[11] A. Atri, J. Amundson, D. Clapham, J. Syned, A single-pool model for intracellular calcium oscillations and waves in the *Xenopus laevis* oocytes, Biophys. J. 65 (1993) 1727–1739.
[12] Y. Tang, J.L. Stephenson, H.G. Othmer, Simplification and analysis of models of calcium dynamics based on IP_3-sensitive calcium channel kinetics, Biophys. J. 70 (1996) 246–263.
[13] D.-O.D. Mak, S. McBride, J.K. Foskett, Inositol 1,4,5-tris-phosphate activation of inositol tris-phosphate receptor Ca^{2+} channel by ligand tuning of Ca^{2+} inhibition, Proc. Natl. Acad. Sci. U. S. A. 95 (1998) 15821–15825.
[14] M. Marhl, S. Schuster, M. Brumen, R. Heinrich, Modeling the interrelations between calcium oscillations and ER membrane potential oscillations, Biophys. Chem. 63 (1997) 221–239.
[15] S. Schuster, M. Marhl, T. Höfer, Modeling of simple and complex calcium oscillations: from single-cell response to intercellular signaling, Eur. J. Biochem. 269 (2002) 1333–1355.
[16] M. Falcke, Reading the patterns in living cells—the physics of Ca^{2+} signaling, Adv. Phys., 53 (2004) 255–440.
[17] P.G. Hogan, A. Rao, Dissecting I_{CRAC}, a store-operated calcium current, Trends Biochem. Sci. 32 (2007) 235–245.
[18] J.W. Putney Jr., Capacitative calcium entry revisited, Cell Calcium 11 (1990) 611–624.
[19] R.S. Lewis, The molecular choreography of a store-operated calcium channel, Nature 446 (2007) 284–287.
[20] A.B. Parekh, J.W. Putney Jr., Store-operated calcium channels, Physiol. Rev. 85 (2005) 757–810.
[21] M. Hoth, R. Penner, Calcium release-activated calcium current in rat mast cells, J. Physiol. 465 (1993) 359–386.
[22] A. Zweifach, R.S. Lewis, Mitogen-regulated Ca^{2+} current of T lymphocytes is activated by depletion of intracellular Ca^{2+} stores, Proc. Natl. Acad. Sci. U. S. A. 90 (1993) 6295–6299.
[23] M. Partiseti, F.L. Deist, C. Hivroz, A. Fischer, H. Korn, D. Choquet, The calcium current activated by T cell receptor and store depletion in human lymphocytes is absent in a primary immunodeficiency, J. Biol. Chem. 269 (1994) 32327–32335.
[24] M. Prakriya, R.S. Lewis, Separation and characterization of currents through store-operated CRAC channels and Mg^{2+}-inhibited cation (MIC) channels, J. Gen. Physiol. 119 (2002) 487–507.
[25] A.M. Hofer, C. Fasolato, T. Pozzan, Capacitative Ca^{2+} entry is closely linked to the filling state of internal Ca^{2+} stores: a study using simultaneous measurements of I_{CRAC} and intraluminal $[Ca^{2+}]$, J. Cell Biol. 140 (1998) 325–334.
[26] S. Feske, R. Draeger, H.H. Peter, K. Eichmann, A. Rao, The duration of nuclear residence of NFAT determines the pattern of cytokine expression in human SCID T cells, J. Immunol. 165 (2000) 297–305.
[27] J. Roos, P.J. DiGregorio, A.V. Yeromin, K. Ohlsen, M. Lioudyno, S. Zhang, O. Safrina, J. A. Kozak, S.L. Wagner, M.D. cahalan, G. Veliçelebi, K.A. Stauderman, STIM1, an essential and conserved component of store-operated Ca^{2+} channel function, J. cell Biol. 169 (2005) 435–445.
[28] J. Liou, M.L. Kim, W.D. Heo, J.T. Jones, J.W. Myers, J.E. Ferrell Jr., T. Meyer, STIM is a Ca^{2+} sensor essential for Ca^{2+}-store-depletion-triggered Ca^{2+} influx, Curr. Biol. 15 (2005) 1235–1241.
[29] S.L. Zhang, Y. Yu, J. Roos, J.A. Kozak, T.J. Deerinck, M.H. Ellisman, K.A. Stauderman, M.D. Cahalan, STIM1 is a Ca^{2+} sensor that activates CRAC channels and migrates from the Ca^{2+} store to the plasma membrane, Nature 437 (2005) 902–905.
[30] J. Soboloff, M.A. Spassova, M.A. Dziadek, D.L. Gill, Calcium signals mediated by STIM and Orai proteins—a new paradigm in inter-organelle communication, Biochim, Biophys. Acta 1763 (2006) 1161–1168.
[31] S. Feske, Y. Gwack, M. Prakriya, S. Srikanth, S.H. Puppel, B. Tanasa, P.G. Hogan, R.S. Lewis, M. Daly, A. Rao, A mutation in Orai1 causes immune deficiency by abrogating CRAC channel function, Nature 441 (2006) 179–185.
[32] R.M. Luik, M.M. Wu, J.A. Buchanan, R.S. Lewis, The elementary unit of store-operated Ca^{2+} entry: local activation of CRAC channels by STIM1 at ER-plasma membrane junctions, J. Cell Biol. 174 (2006) 815–825.
[33] T.A. Rooney, E.J. Sass, A.P. Thomas, Characterization of cytosolic calcium oscillations induced by phenylephrine and vasopressin in single fura-2-loaded hepatocytes, J. Biol. Chem. 264 (1989) 17131–17141.
[34] A.V. Yeromin, S.L. Zhang, W. Jiang, Y. Yu, O. Safrina, M.D. Cahalan, Molecular identification of the CRAC channel by altered ion selectivity in a mutant of Orai, Nature 443 (2006) 226–229.
[35] J.C. Mercer, W.I. DeHaven, J.T. Smyth, B. Wedel, R.R. Boyles, G.S. Bird, J.W. Putney Jr., Large store-operated calcium selective currents due to co-expression of Orai1 or Orai2 with the intracellular calcium sensor, STIM1, J. Biol. Chem. 281 (2006) 24979–24990.
[36] M. Prakriya, S. Feske, Y. Gwack, S. Srikanth, A. Rao, P.G. Hogan, Orai1 is an essential pore subunit of the CRAC channel, Nature 443 (2006) 230–233.
[37] C. Peinelt, M. Vig, D.L. Koomoa, A. Beck, M.J.S. Nadler, M.K. Huberson, A. Lis, A. Fleig, R. Penner, J.P. Kinet, Amplification of CRAC current by STIM1 and CRACM1 (Orai1), Nat. Cell Biol. 8 (2006) 771–773.
[38] J.M. Kowalewski, P. Uhlén, H. Kitano, H. Brismar, Modeling the impact of store-operated Ca^{2+} entry on intracellular Ca^{2+} oscillations, Math. Biosci. 204 (2006) 232–249.
[39] H.L. Baker, R.J. Errington, S.C. Davies, A.K. Campbell, A mathematical model predicts that calreticulin interacts with the endoplasmic reticulum Ca^{2+}-ATPase, Biophys. J. 82 (2002) 582–590.
[40] M.J. Berridge, M.D. Bootman, H.L. Roderick, Calcium signaling: dynamics, homeostasis and remodeling, Nat. Rev. Mol. Cell Biol. 4 (2003) 517–529.
[41] C.P. Fall, E.S. Marland, J.M. Wagner, J.J. Tyson, Computational Cell Biology, New York, 2002.
[42] M.M. Wu, J. Buchanan, R.M. Luik, R.S. Lewis, Ca^{2+} store depletion causes SITM1 to accumulate in ER regions closely associated with the plasma membrane, J. Cell Biol. 174 (2006) 803–813.
[43] P.B. Stathopulos, G.Y. Li, M.J. Plevin, J.B. Ames, M. Ikura, Stored Ca^{2+} depletion-induced oligomerization of stromal interaction molecule 1 (STIM1) via the EF-SAM region, J. Biol. Chem. 281 (2006) 35855–35862.
[44] M. Vig, A. Beck, J.M. Billingsley, A. Lis, S. Parvez, C. Peinelt, D.L. Koomoa, J. Soboloff, D.L. Gill, A. Fleig, J.P. Kinet, R. Penner, CRACM1 multimers form the ion-selective pore of the CRAC channel, Curr. Biol. 16 (2006) 2073–2079.
[45] J.L. Blank, A.H. Ross, J.H. Exton, Purification and characterization of two G-protein that activate the beta-1 isozyme of phosphoinositede-specific phospholipase C, J. Biol. Chem. 266 (1991) 18206–18216.
[46] C.W. Taylor, Store-operated Ca^{2+} entry: a STIMulation stOrai, Trends Biochem. Sci. 31 (2006) 597–601.
[47] H.L. Ong, X. Liu, K.T. Atanasova, B.B. Singh, B.C. Bandyopadhyay, W.D. Swaim, J.T. Russell, R.S. Hegde, A. Sherman, I.S. Ambudkar, Relocalization of STIM1 for activation of store-operated Ca^{2+} entry is determined by the depletion of subplasma membrane endoplasmic reticulum Ca^{2+} store, J. Biol. Chem. 282 (2007) 12176–12185.
[48] T.J. Shuttleworth, Receptor-activated calcium entry channels—who does what, and when? Sci. STKE 243 (2004) pe40.
[49] G.S. Bird, J.W. Putney Jr., Capacitative calcium entry supports calcium oscillations in human embryonic kidney cells, J. Physiol. 562 (2005) 697–706.
[50] M. Vig, C. Peinelt, A. Beck, D.L. Koomoa, D. Rabah, M.K. Huberson, S. Kraft, H. Turner, A. Fleig, R. Penner, J.P. Kinet, CRACM1 is a plasma membrane protein essential for store-operated Ca^{2+} entry, Science 312 (2006) 1220–1223.
[51] A.P. Thomas, G.J. Bird, G. Hajnóczky, L.D. Robb-Gaspers, J.W. Putney Jr., Spatial and temporal aspects of cellular calcium signaling, FASEB J. 10 (1996) 1505–1517.
[52] N.M. Woods, C.J. Dixon, K.S. Cuthbertson, P.H. Cobbold, Modulation of free Ca oscillations in single hepatocytes by changes in extracellular K^+, Na^+ and Ca^{2+}, Cell Calcium 11 (1990) 353–360.
[53] M. Grimaldi, M. Maratos, A. Verma, Transient receptor potential channel activation causes a novel form of $[Ca^{2+}]_i$ oscillations and is not involved in capacitative Ca^{2+} entry in glial cells, J. Neurosci. 23 (2003) 4737–4745.
[54] X. Wu, G. Babnigg, T. Zagranichnaya, M.L. Villereal, The role of endogenous human trp4 in regulating carbachol-induced calcium oscillations in HEK-293 cells, J. Biol. Chem. 277 (2002) 13597–13608.
[55] S. Barg, X. Ma, L. Eliasson, J. Galvanovskis, S.O. Göpel, S. Obermüller, J. Platzer, E. Renström, M. Trus, D. Atlas, J. Striessnig, P. Rorsman, Fast exocytosis with few Ca^{2+} channels in insulin-secreting mouse pancreatic B Cells, Biophys. J. 81 (2001) 3308–3323.
[56] M. Wakui, B.V.L. Potter, O.H. Petersen, Pulsatile intracellular calcium release does not depend on fluctuations in inositol trisphosphate concentration, Nature 339 (1989) 317–320.
[57] J.D. Lechleiter, D.E. Clapham, Molecular mechanism of intracellular calcium excitability in *X. laevis* oocytes, Cell 69 (1992) 283–294.
[58] G. Hajnóczky, A.P. Thomas, Minimal requirements for calcium oscillations driven by the IP_3 receptor, EMBO J. 16 (1997) 3533–3543.
[59] B. Zimmermann, B. Walz, The mechanism mediating regenerative intercellular Ca^{2+} waves in the blowfly salivary gland, EMBO J. 18 (1999) 3222–3231.
[60] U. Kummer, L.F. Olsen, C.J. Dixon, A.K. Green, E. Bornberg-Bauer, G. Baier, Switching from simple to complex oscillations in calcium signaling, Biphys. J. 79 (2000) 1188–1195.
[61] M.S. Nash, K.W. Young, R.A.J. Challiss, S.R. Nahorski, Intracellular signalling: Receptor-specific messenger oscillations, Nature, 413 (2001) 381–382.